Available online at www.sciencedirect.com
SCIENCE DIRECT®
Physica D 195 (2004) 292–302
PHYSICA D
www.elsevier.com/locate/physd

Analytical search for bifurcation surfaces in parameter space

Thilo Gross*, Ulrike Feudel

ICBM, Carl von Osssietzky Univerität, PF 2503, 26111 Oldenburg, Germany

Received 14 November 2002; received in revised form 1 March 2004; accepted 23 March 2004
Communicated by E. Kostelich

Abstract

The method of resultants can be used to compute Hopf bifurcations in ODE systems. We discuss this method from the applicant's point of view. Furthermore, we show by theory and examples that the method may be extended to cover other bifurcation situations as well. Among them are the real Hopf situation, which plays an important role in the transition to Shil'nikov chaos as well as some higher codimension bifurcations, such as Takens–Bogdanov, Gavrilov–Guckenheimer, and double Hopf bifurcations. The method yields an analytical test function that can be solved analytically or by computer algebra systems. In contrast to common analytical techniques based on eigenvalue computation (which can only be applied to systems of size $N \leq 4$), the method is applicable for systems of intermediate size ($N < 10$). We illustrate the power of the method by discussing examples from different disciplines of science: a Lorenz-like oscillator, two coupled oscillators, and a five-species food chain.

PACS: 05.45.−a

Keywords: Bifurcation detection; Hopf bifurcation; Higher codimension bifurcations

1. Introduction

The time evolution of natural systems displays a large variety of qualitatively different long-term behaviors. The system's long-term dynamics can be either stationary, periodic, quasiperiodic, or chaotic. If environmental parameters (such as ambient temperature) are varied, a change in the system's behavior is likely to occur. Even a small, gradual variation of the parameters may induce a sudden, discontinuous change in the system's long-term dynamics. The critical threshold values at which this happens are called bifurcations. Crossing a bifurcation is related to an *instability* of a certain long-term behavior. Depending on the nature of the transition, one can distinguish between different types of bifurcations. For example, at a Hopf bifurcation [1], a transition from stationary to periodic motion occurs, while at a Neĭmark–Sacker bifurcation, a transition from periodic to quasiperiodic motion takes place [2,3].

The presence of a bifurcation is of great importance in many physical, chemical, and biological systems. For instance, the formation of Rayleigh–Bénard convection cells in hydrodynamics [4], the onset of Belousov–Zhabotinsky oscillations in chemistry [5], the occurrence of spikes in neuron models [6], and the breakdown of the thermohaline ocean circulation in climate dynamics [7,8] are caused by crossing Hopf bifurcations.

* Corresponding author. Fax: +49-441-798-3404.
E-mail address: thilo.gross@physics.org (T. Gross).

0167-2789/$ – see front matter
doi:10.1016/j.physd.2004.03.019

In this paper, we focus on bifurcations in the large class of model systems that consist of N variables $x_1, \ldots, x_N$, the dynamics of which is given by N ordinary differential equations (ODEs) of the form

$$\dot{x}_i = F_i(x_1, \ldots, x_N, p_1, \ldots, p_M), \quad i = 1, \ldots, N. \quad (1)$$

The functions $F_1, \ldots, F_N$ are in general nonlinear in $x_1, \ldots, x_N$ and depend on M parameters $p_1, \ldots, p_M$. The form of these functions determines the type and location of the bifurcations encountered.

To locate the bifurcations of a given system in parameter space is one of the main tasks of qualitative analysis. One can distinguish between local and global bifurcations [9,10]. While global bifurcations cannot be detected by a local stability analysis, local bifurcations correspond to qualitative changes in the neighborhood of one steady state and can, therefore, be detected by monitoring the eigenvalues of the corresponding Jacobian matrix. This is usually done by numerically solving a system of nonlinear equations designed in a way that they yield the bifurcation point as a unique solution [11–13].

While several software packages for the convenient computation of bifurcations exist [14–18], these are only capable of calculating bifurcations as a function of up to two parameters. In many practical applications, however, one is interested in the whole parameter space. Therefore, an analytical approach that can yield the bifurcation as a function of all system parameters is highly desirable. Direct analytical computation of the eigenvalues is possible only for small systems up to $N = 4$. However, the knowledge of all eigenvalues is not always necessary for bifurcation detection. Consider for instance transcritical, pitchfork, or turning-point bifurcations. These bifurcations occur if an eigenvalue of the Jacobian becomes zero. The determinant of the Jacobian can therefore act as a test function for such bifurcations. Checking for a vanishing determinant in general is much easier than the factorization of the Jacobian's characteristic polynomial and is possible for systems of any size.

Two methods that yield analytical test functions for the Hopf bifurcation have been proposed in [19]. One of these is the method of resultants. The basic idea of this method is that the symmetry of the eigenvalues may be used to split the characteristic polynomial of the Jacobian matrix into two coupled polynomials. Unlike a single polynomial, two coupled polynomials may always be solved using resultants. In this paper, we show by theory and examples that this method is not only applicable to Hopf bifurcation points but also that it may be used to compute other interesting bifurcation situations, like real Hopf, Takens–Bogdanov, Gavrilov–Guckenheimer, and double Hopf bifurcations. The method is especially advantageous for systems of intermediate size (say, $N < 10$) for which an analytical test function with full parameter dependence can be obtained. In smaller systems, these test functions can often be solved to yield an explicit description of the bifurcation surfaces.

The paper is organized as follows. The bifurcations for which the method can be used are explained in detail in Section 2. In Section 3, we give an outline of the method showing how properties of the bifurcations can be used to derive a suitable test function. Three examples are presented in Section 4. We start with a Lorenz-like Shimizu–Morioka oscillator. In the second example, two of these oscillators are coupled to yield a six-dimensional system. Finally, we investigate the bifurcations of an example from population dynamics, namely a five-species food chain. We finish in Section 5 with conclusions underlining the usefulness of this approach for small and intermediate-size systems and discuss possible extensions of the method.

2. Tractable bifurcations

The method of resultants was originally proposed for the computation of Hopf bifurcations [19]. However, the method is applicable to many bifurcation situations, of which Hopf, Takens–Bogdanov, Gavrilov–Guckenheimer, and double Hopf bifurcations are the most important. They are known to occur in many physical systems and often play an important role for the systems' long-term behavior. At the bifurcation point, the dynamics of the system changes in a typical way depending on the type of bifurcation involved. In this section, we discuss these particular bifurcations and their effects on model dy-

namics. At the end of the section, we describe an interesting eigenvalue constellation known as the real Hopf situation, which can as well be detected using the proposed method.

In a *Hopf* bifurcation, a pair of complex conjugate eigenvalues of the Jacobian crosses the imaginary axis. If the system is in a stable steady state before the bifurcation, then the steady state loses its stability at the bifurcation point. Furthermore, a stable or unstable limit cycle either emerges or vanishes in the Hopf bifurcation. In the long-term behavior, the Hopf bifurcation of a stable steady state is reflected by a transition between stationary and periodic behavior.

Since the method is used to detect the Hopf bifurcation with full parameter dependence, higher codimension bifurcations that involve a Hopf bifurcation can be detected easily. For instance, the *Takens–Bogdanov* (TB) bifurcation is a codimension-2 bifurcation in which a branch of Hopf bifurcations vanishes as the steady state of interest undergoes a turning point (saddle-node) bifurcation. Furthermore, a branch of homoclinic bifurcations emerges from this bifurcation. The homoclinic bifurcation will be discussed later in this section. At the TB point, the Jacobian of the system has a double zero eigenvalue.

Another example of a codimension-2 bifurcation is the *Gavrilov–Guckenheimer* (GG) bifurcation. This bifurcation occurs if a Hopf bifurcation meets a transcritical bifurcation. At the bifurcation point, we have a single zero eigenvalue in addition to a purely imaginary eigenvalue pair. Like the TB bifurcation, the GG bifurcation indicates the presence of a branch of homoclinic bifurcations.

Finally, if two Hopf bifurcations meet in parameter space, a codimension-2, *double Hopf* (DH) bifurcation is formed. In this bifurcation, we find two purely imaginary pairs of complex conjugate eigenvalues.

The DH and GG bifurcations are very complex and have not been studied completely [9]. However, their existence in a given system implies the presence of many possible long-term behaviors like stationary, periodic, quasi-periodic, and chaotic behavior.

In contrast to the other bifurcations discussed here, the homoclinic bifurcation is a global bifurcation and cannot be detected by a local stability analysis. However, we have seen that the existence of a homoclinic bifurcation in many cases can be inferred from the presence of a Gavrilov–Guckenheimer or Takens–Bogdanov bifurcation. In a homoclinic bifurcation, a limit cycle emerges from a homoclinic orbit (a trajectory that tends to the same saddle point for $t \to \infty$ and $t \to -\infty$). The stability of the created limit cycle is determined by the eigenvalues of the Jacobian at the saddle point [20]. Knowing the eigenvalue λ_+ with the smallest positive real part and the eigenvalue λ_- with the largest negative real part, the stability of the limit cycle can be expressed in terms of the *saddle index*

$$s = -\frac{\mathrm{Re}(\lambda_-)}{\mathrm{Re}(\lambda_+)}. \tag{2}$$

In this paper, we focus mainly on the case in which both λ_+ and λ_- are real and λ_+ is the only eigenvalue with positive real part. In this case, only a single limit cycle is formed, which is stable if $s > 1$ and unstable if $s < 1$. For $s = 1$, the stability is undetermined, as λ_+ and λ_- are symmetrical with respect to the point of origin.

A situation in which two purely real, symmetric eigenvalues are present is called a *real Hopf* situation [21]. This situation is not to be confused with the (imaginary) Hopf bifurcation, where we have a symmetric but purely imaginary eigenvalue pair. In contrast to the Hopf bifurcation, the real Hopf situation is technically no bifurcation, since it does not necessarily involve the creation or destruction of invariant sets or a change in their stability. However, in systems in which homoclinic bifurcations exist, a real Hopf situation may mark a line of unit saddle index, which may in turn indicate a change in the stability of the limit cycle created in the homoclinic bifurcation.

A similar but less frequently encountered situation is a symmetric pair of complex conjugate eigenvalue pairs. In the following, we call this situation the *complex Hopf* situation. Like the real Hopf situation, it indicates a unit saddle index if no other eigenvalue with real part closer to zero is present, which in turn indicates a change in the limit cycle stability if all other eigenvalues have negative real part.

3. Outline of the method

In this section, we show how the symmetry of some eigenvalues of the Jacobian can be used to detect bifurcations. As a result, we can find an implicit equation that acts as a test function for the bifurcation as well as the values of the symmetric eigenvalues. Explicit calculation of the other eigenvalues is not necessary.

In this section, we largely follow the approach of Guckenheimer et al. [19], although with a different focus. We consider the application of the resultants, not in a numerical but in a computer-algebra-based method. At the end of this section, we summarize our results in algorithmic form to make the application of the method easier.

We consider characteristic polynomials of the form

$$P(\lambda) = \sum_{n=0}^{N} c_n \lambda^n = 0. \tag{3}$$

The common feature of the bifurcations discussed in Section 2 (apart from the homoclinic bifurcation) is the existence of a pair of eigenvalues λ_+ and λ_- satisfying the symmetry condition

$$\lambda_+ = -\lambda_-. \tag{4}$$

For λ_+, Eq. (3) reads

$$P(\lambda_+) = \sum_{n=0}^{N} c_n \lambda_+^n = 0, \tag{5}$$

while for λ_-, Eq. (3) may be written as

$$P(\lambda_-) = \sum_{n=0}^{N} c_n \lambda_+^n (-1)^n = 0. \tag{6}$$

By forming the sum and the difference of Eqs. (5) and (6), we obtain the conditions

$$\sum_{n=0}^{N} c_n (1 + (-1)^n) \lambda_+^n = 0, \tag{7}$$

$$\sum_{n=0}^{N} c_n (1 - (-1)^n) \lambda_+^n = 0. \tag{8}$$

Eq. (7) contains only terms that are of even order in λ_+, while Eq. (8) contains only terms of odd order. Assuming that $\lambda_+ \neq 0$ holds, we divide Eq. (8) by λ_+ and obtain

$$\sum_{n=1}^{N} c_n (1 - (-1)^n) \lambda_+^{n-1} = 0.$$

By dividing once by λ_+, we have insured that the resulting equation cannot be solved by a single zero eigenvalue. However, a double zero eigenvalue (for instance at a TB point) can still solve the equation.

Having eliminated all terms with odd orders in λ_+, we may reduce the order of the polynomials by the substituting the Hopf number [21]

$$\chi := \lambda_+^2, \tag{9}$$

which yields

$$\sum_{n=0}^{N/2} c_{2n} \chi^n = 0, \tag{10}$$

$$\sum_{n=0}^{N/2} c_{2n+1} \chi^n = 0, \tag{11}$$

where $N/2$ has to be rounded up or down to an integer value as required. So far, we have split the characteristic polynomial of order N into two coupled polynomials of order $N/2$ by employing the symmetry condition. Using results from mathematical elimination theory [22], we know that two general polynomials $f(x)$ and $g(x)$ have a common root if the resultant $R(f, g)$ of the two polynomials vanishes. Using the Sylvester formula, the resultant of Eqs. (10) and (11) can be written in Hurwitz form

$$R_N := \begin{vmatrix} c_1 & c_0 & 0 & \dots & 0 \\ c_3 & c_2 & c_1 & \dots & 0 \\ \vdots & \vdots & \vdots & \ddots & \vdots \\ c_N & c_{N-1} & c_{N-2} & \dots & c_0 \\ 0 & 0 & c_N & \dots & c_2 \\ 0 & 0 & 0 & \dots & c_4 \\ \vdots & \vdots & \vdots & \ddots & \vdots \\ 0 & 0 & 0 & \dots & c_{N-1} \end{vmatrix}. \tag{12}$$

For sake of simplicity, we have assumed that N is odd.

The formulation of the resultant is an important step in the method. To make this step easier, we would like

to provide the reader with a simple algorithm: take a determinant of size $(N-1)\times(N-1)$. Let the first element of the first row be c_1. If the first element of a given row is c_n, then the first element of the next row is c_{n+2}. If an element is c_n, then the next element in the same row is c_{n-1}. Use these rules to fill the whole determinant. Finally, set all coefficients that do not appear in the characteristic polynomial (such as c_{-1}) to zero.

For example, the resultant for $N=6$ is

$$R_6 = \begin{vmatrix} c_1 & c_0 & 0 & 0 & 0 \\ c_3 & c_2 & c_1 & c_0 & 0 \\ c_5 & c_4 & c_3 & c_2 & c_1 \\ 0 & c_6 & c_5 & c_4 & c_3 \\ 0 & 0 & 0 & c_6 & c_5 \end{vmatrix}. \tag{13}$$

So far we have shown that, to check for the symmetry condition which indicates many interesting bifurcations, one has only to compute the value of the resultant. Although the calculation of large determinants can be tedious, it is much easier than the factorization of the characteristic polynomial. To determine which of the bifurcation situations mentioned in Section 2 has been encountered, we need to find the value of the Hopf number χ.

It has been proved [22] that unless all partial derivatives of the resultant vanish the common root of two polynomials can always be found from the proportions

$$(1:\chi:\cdots:\chi^N) = \left(\frac{\partial R_N}{\partial c_0} : \frac{\partial R_N}{\partial c_2} : \cdots : \frac{\partial R_N}{\partial c_{N-1}}\right),$$
$$(1:\chi:\cdots:\chi^N) = \left(\frac{\partial R_N}{\partial c_1} : \frac{\partial R_N}{\partial c_3} : \cdots : \frac{\partial R_N}{\partial c_N}\right).$$

A more efficient way to find the common root goes as follows. For systems with $N>3$, delete the last two columns and the last row of the resultant matrix, yielding a $(N-3)\times(N-2)$ matrix A. Then, generate a $(N-3)\times(N-3)$ matrix B by deleting an arbitrary row j (say, row 1) of A. Generate another $(N-3)\times(N-3)$ matrix C by deleting row $j+1$ of the matrix A. The common root can now be computed as

$$\chi = -\frac{|B|}{|C|}. \tag{14}$$

For systems with $N=3$ or $N=2$, the common root is simply

$$\chi = -\frac{c_0}{c_2}. \tag{15}$$

We consider the example $N=6$ again, which yields (for $j=1$)

$$\chi = -\frac{\begin{vmatrix} c_1 & c_0 & 0 \\ c_5 & c_4 & c_3 \\ 0 & c_6 & c_5 \end{vmatrix}}{\begin{vmatrix} c_3 & c_2 & c_1 \\ c_5 & c_4 & c_3 \\ 0 & c_6 & c_5 \end{vmatrix}}.$$

So far we have shown that a symmetric eigenvalue pair exists if the resultant given by Eq. (12) vanishes. We can compute the Hopf number χ, which is the square of the symmetric eigenvalues, by applying Eq. (14) or Eq. (15). Knowing χ, we can distinguish between four different situations:

- χ real, <0 (Hopf bifurcation).
- χ real, >0 (real Hopf situation).
- χ undetermined (more complex situations (e.g., double Hopf)).
- $\chi=0$ (Takens–Bogdanov point).

Note that the common root may be undetermined if $|C|=0$ and $|A|=0$. However, such situations are at least of codimension-2 and therefore rarely encountered.

Furthermore, we have to emphasize that the method detects eigenvalue constellations that do not always necessarily alter the long-term behavior of the system. Whether the long-term behavior is altered depends on the other eigenvalues, which are not calculated explicitly. Therefore, simulations should be carried out to determine how the long-term behavior is affected. However, since the potential bifurcation surfaces are known, one simulation run on either side of the surface is usually sufficient to find out whether and how the dynamics of the system change at the surface.

Summing up the results of this section, we can identify the following key steps in the method:

(1) Calculate the coefficients $c_0, \ldots, c_N$ of the characteristic polynomial.
(2) Derive an implicit equation describing the bifurcation by demanding that the resultant be zero.
(3) Calculate χ using Eq. (14) to determine the type of the bifurcation.
(4) Plot the bifurcation surface, solving the implicit condition analytically or numerically.
(5) Locate higher codimension bifurcations in the plot.

4. Examples

Although it is easy to implement, the method of resultants has, to our knowledge, rarely been applied (see [23]). In this section, we present three examples by which we aim to underline the advantages of the method. Since the method is very general in nature, we had to choose from a wide range of possible applications. The first example has been chosen to illustrate the extension to the real Hopf situation. The second example proves the applicability of the method to systems of intermediate size. Finally, the appearance of higher codimension bifurcations is shown in the third example.

The first two examples deal with an extended Shimizu–Morioka oscillator, which is a Lorenz-like system that turns up in fluid dynamics as well as in laser physics. In the first example, we study a single oscillator. Since the oscillator is only three-dimensional, its Hopf bifurcations can be found by explicit calculation of the eigenvalues of the Jacobian. However, even in this simple case, the method of resultants is more convenient. We include this easy example because it illustrates the spirit of the method very well. Furthermore, it serves as an introduction to the second example, in which we demonstrate the applicability of the method for larger ($N = 6$) systems by considering two coupled Shimizu–Morioka oscillators. Our final example deals with an ecosystem model of five species that interact in a five-level food chain. This example has been chosen because it originates from yet another branch of science and contains interesting bifurcations of higher codimension.

4.1. Extended Shimizu–Morioka model

The well-known Lorenz model was originally developed to describe Bénard convection in a heated fluid [10]. The dynamics of the three model variables x, y, and z are given by

$$\dot{x} = -\sigma(x - y),$$
$$\dot{y} = rx - y - xz,$$
$$\dot{z} = -bz + xy.$$

The parameter r is the relative Rayleigh number, σ the Prandtl number, and b is a constant depending on the geometry of the convection cell. In this example, we study the behavior of the Lorenz-like extended Shimizu–Morioka model [24]

$$\dot{x} = y,$$
$$\dot{y} = x(1 - z) - Bx^3 - ly,$$
$$\dot{z} = -a(z - x^2).$$

This model is a reduced version of the Lorenz model for $r > 1$. The parameters of the two models are related by

$$a = \frac{b}{\sqrt{\sigma(r-1)}},$$
$$l = \frac{\sigma + 1}{\sqrt{\sigma(r-1)}},$$
$$B = \frac{b}{2\sigma - b}.$$

For $B = 0$, the extended model is identical to the original Shimizu–Morioka model, which was introduced as a approximation to the Lorenz model for high Rayleigh numbers [25].

Apart from their important role in fluid dynamics, Lorenz and Lorenz-like systems turn up in many different areas of physics. The Shimizu–Morioka model has been shown to be a low-dimensional model of the zero-intensity state of lasers containing a saturable absorber [24]. The extended model exhibits dynamics that are similar to some three-level laser models. More generally speaking, it can serve as a truncated asymptotic normal form (that is, a low-dimensional approximation) of a class of higher-dimensional models. In this case, B is a constant that depends on the specific structure of the higher-dimensional system.

The dynamics of the extended Shimizu–Morioka oscillator have been studied numerically [24] and analytically using the method of comparison systems [26]. The investigations show that a Hopf bifurcation and a surface of unit saddle index are involved in the creation of a large region of Shil'nikov chaos in parameter space.

The system has one trivial steady state with $x = 0$ and two symmetric non-trivial steady states with $x = \pm(1 + B)^{-1/2}$. In all steady states, $y = 0$ and $z = x^2$ hold. In the nontrivial steady states, we obtain the characteristic polynomial

$$\lambda^3 + (a + l)\lambda^2 + (al + 2B(B + 1)^{-1})\lambda + 2a = 0.$$

The resultant according to Eq. (12) is

$$\begin{vmatrix} la + 2B(B + 1)^{-1} & 2a \\ 1 & a + l \end{vmatrix} = 0,$$

yielding

$$B = -\frac{la(l + a) - 2a}{la(l + a) + 2l}. \tag{16}$$

The Hopf number on the bifurcation line given by Eq. (15) is

$$\chi = -\frac{2a}{a + l}.$$

Since χ is negative for $a > 0$ and $l > 0$, the surface described by Eq. (16) is a Hopf bifurcation.

An analogous investigation of the trivial steady state reveals a real Hopf situation, corresponding to a unit saddle index surface at

$$l = a^{-1} - a^2$$

for arbitrary B.

The surfaces are shown in Fig. 1. Both surfaces play an important role in the formation of the chaotic region. The chaotic attractor is formed from a pair of limit cycles that emerge from the nontrivial steady state in the Hopf bifurcation and undergo a homoclinic bifurcation with the trivial steady state, which is (mainly) encountered below the Hopf (dark gray) surface and to the left of the real Hopf situation (light gray). Therefore, the system may be regarded as more stable if the Hopf bifurcation happens at a low value of l.

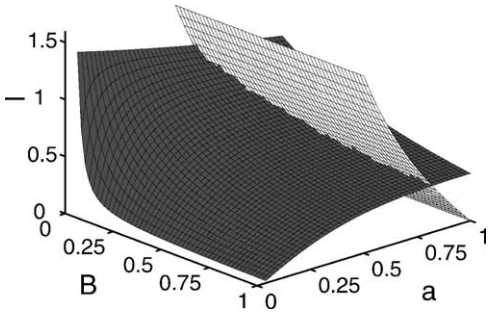

Fig. 1. The Hopf (dark gray) and the real Hopf situation (light gray) surface of Shimizu-Morioka oscillator depending on the three parameters a, B, and l.

Increasing B rapidly stabilizes the system by lowering the critical value of l. For $B = 0$, increasing a stabilizes the system, but only so slightly that hardly any decrease in l is visible in the figure. Even at very small values of B, the system is no longer stabilized by increasing a, as the critical l now increases as a is increased.

Using the proposed method, the bifurcation surfaces have been found in minutes. In comparison, the analytic factorization of the characteristic polynomial and subsequent search for symmetric or purely imaginary eigenvalues is a much more tedious task.

4.2. Coupled oscillators

In our next example, we study a system of two coupled oscillators of the type discussed in Section 4.1. For the sake of simplicity, we apply the coupling in the y direction. In this way, the coupling does not alter the steady state values of the individual oscillators, since the coupling term vanishes in all individual steady states.

We obtain the ODE system

$$\begin{aligned}
\dot{x}_1 &= y_1, \\
\dot{y}_1 &= x_1(1 - z_1) - Bx_1^3 - ly_1 - k(y_1 - y_2), \\
\dot{z}_1 &= -a(z_1 - (x_1)^2), \\
\dot{x}_2 &= y_2, \\
\dot{y}_2 &= x_2(1 - z_2) - Bx_2^3 - ly_2 + k(y_1 - y_2), \\
\dot{z}_2 &= -a(z_2 - (x_2)^2),
\end{aligned}$$

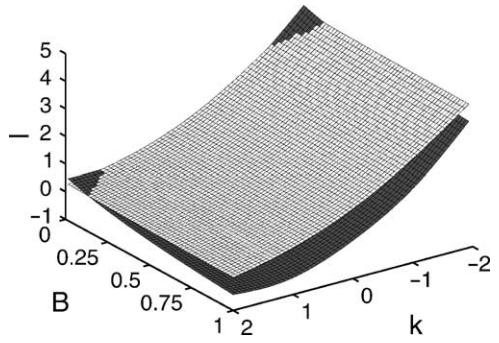

Fig. 2. Hopf (dark gray) and real Hopf situation (light gray) surfaces of the coupled oscillator system depending on the nonlinearity B and coupling strength k at $a = 0.5$.

where k is the coupling strength. This system has not been chosen with any specific application in mind. Rather, it should be viewed as a simple but realistic example of a coupled oscillator system.

In this paper, our aim is not to give a exhaustive discussion of the behavior of the system, which would require the investigation of the dynamics around all steady states as well as further analysis. To give a brief demonstration of the usefulness of the method, we restrict ourselves to the investigation of the steady states in which one oscillator is in a trivial state and another oscillator is in a nontrivial state. This case proves to be particularly interesting, since both bifurcation surfaces found in our earlier example reappear.

Since the system is six-dimensional, the eigenvalues of the Jacobian cannot be calculated analytically. Using the method of resultants, however, an implicit condition for the bifurcation surfaces can still be derived using symbolic mathematics tools like Maple and Mathematica. The analysis reveals a Hopf bifurcation surface and a surface of unit saddle index, shown in Fig. 2. Although the result obtained with the method has full parameter dependence, we have set $a = 0.5$ to be able to display the results in a convenient form.

The results obtained by the method of resultants are shown in Fig. 2. As in the single oscillator case, we find a Hopf bifurcation surface (dark gray) and a real Hopf situation surface (light gray). Again, the chaotic region is encountered mainly below the Hopf bifurcation. Since the critical value of l decreases as k is increased, the system is stabilized by positive coupling.

4.3. Five-level food chain

The dynamics of ecosystem models is of great interest in theoretical ecology. A knowledge of the mechanisms that lead to the initial loss of stability of the steady state and of the parameter values at which this loss occurs helps environmental scientists to evaluate proposed measures for stabilizing endangered ecosystems. In this example, we study a simple food chain model.

A food chain is a system consisting of a number of species that occupy different trophic levels. The lowest trophic level is held by the primary producer of biomass. The species that preys on the primary producer occupies the second level, and so on. Short food chains of up to three species have often been studied in theoretical ecology (see, for instance, [27]). However, in nature, food chains of length up to six have been observed.

In this example, we study a five-level food chain, since this case proves to be especially interesting. The abundance of the five species is described by the variables $X_1, \ldots, X_5$ whose index denotes the trophic level. The dynamics of the model are given by

$$\begin{aligned}
\dot{X}_1 &= \tilde{g}(X_0)X_1 - g(X_1)X_2,\\
\dot{X}_2 &= r^1(g(X_1)X_2 - g(X_2)X_3),\\
\dot{X}_3 &= r^2(g(X_2)X_3 - g(X_3)X_4),\\
\dot{X}_4 &= r^3(g(X_3)X_4 - g(X_4)X_5),\\
\dot{X}_5 &= r^4(g(X_4)X_5 - X_5).
\end{aligned} \tag{17}$$

In these equations, we have assumed that the rate of predation is linear in the predator abundance and in some function g of the prey abundance. Species X_1 feeds on a nutrient source X_0, the concentration of which is given by the algebraic equation

$$X_0 = K - X_1, \tag{18}$$

where K is a carrying capacity that describes the total amount of nutrients in the system. Apart from predation, no other loss terms arise except for the top predator X_5, which has a linear mortality due to natural death, disease, or predation by higher species that are not modeled explicitly.

By scaling the species abundances and time appropriately, the system has been normalized such that

$$\tilde{g}(X_0^*) = \tilde{g}(K-1) = 1, \tag{19}$$

$$g(X_i^*) = g(1) = 1, \quad i > 0. \tag{20}$$

Here $X_1^*, \ldots, X_5^*$ denote the abundances in the normalized steady state $X_i = 1$, $i = 1, \ldots, 5$. There is at least one other nontrivial steady state, and more may arise depending on the form of g and $\tilde{g}$.

Higher trophic levels are generally occupied by species with larger individuals. Since larger animals have in general a longer lifecycle, a slowing down of the growth rates with increasing trophic level is observed in almost all food chains. This slowing down is modeled by including increasing powers of r in Eqs. (17).

As a result, Eqs. (17) are a simple but fairly realistic model of a five-trophic foodchain. The reason for choosing this specific model is that it can be described entirely by the parameter r and the parameters

$$a = \left.\frac{\partial \tilde{g}}{\partial X_0}\right|_{X_0 = X_0^*}, \qquad h = \left.\frac{\partial g}{\partial X_i}\right|_{X_i = X_i^*}, \quad i > 0.$$

In contrast, most other food chain models contain many more parameters. More parameters pose no problem to the method but may confuse a general audience. The parameters a and h measure the slope of the interaction functions in the steady state, which allows us to simulate the effect of different types of functions $g(\cdot)$. In Lotka–Volterra models, g is assumed to be linear. In this case, $h = 1$ because of Eq. (20). More realistic models use functions of Holling type that are linear for small prey abundance but approach a limit as the prey abundance grows.

The value of parameter a contains the carrying capacity K implicitly. Due to Eq. (18), large a implies that the amount of nutrients that can be harvested by the primary producer decreases rapidly as X_1 increases over the steady state value. This will in general be the case in environments with low carrying capacity, while $a \approx 0$ will only be found in environments with infinite carrying capacity. The parameter r in general is chosen such that $0 \leq r \leq 1$ to slow down the higher species.

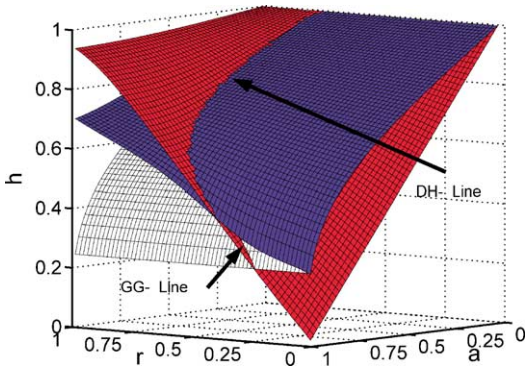

Fig. 3. Bifurcations of the five-level food chain. The two dark surfaces correspond to Hopf bifurcations, while the white surface in general is a transcritical bifurcation. A double Hopf (DH) bifurcation line is formed at the intersection of the dark surfaces. Furthermore, there is a Gavrilov–Guckenheimer (GG) bifurcation line at the intersection of one of the dark surfaces with the white surface.

The system described by Eqs. (17) is numerically difficult to handle because of the different time scales that arise for small values of r. Applying the method, we obtain the bifurcation diagram shown in Fig. 3. The gray surfaces shown in the picture are Hopf bifurcations. On the white surface, the determinant of the Jacobian vanishes. This surface in general corresponds to a transcritical bifurcation (depending on g and $\tilde{g}$). The steady state is stable above the surfaces, and, if h is decreased, becomes unstable in a Hopf bifurcation. Thereafter, the other two bifurcations are encountered, in which the steady state stays unstable. Where the two Hopf surfaces intersect, a double Hopf (DH) bifurcation is formed. Furthermore, there is a Gavrilov–Guckenheimer (GG) bifurcation line at the intersection of one of the Hopf bifurcation surfaces with the transcritical bifurcation. All three bifurcation surfaces meet in a single line at $a = 0$ and $h = 1$, which corresponds for instance to a Lotka–Volterra food chain in an environment with infinite carrying capacity. On this line, we have five eigenvalues with vanishing real part.

These results demonstrate that food chains of the given form are stable if the predators are sensitive enough to prey density (high h). Stability is improved if the carrying capacity of the environment is low (high a) while stability is reduced in nutrient-rich environ-

ments (low a). Food chains in which predators grow nearly as fast as their prey (r close to 1) are generally likely to become unstable regardless of the carrying capacity.

The dynamics of the five-level food chain are an example of the so-called paradox of enrichment [28]. In general, an attempt to enrich an ecosystem by adding nutrients fails. An increased amount of nutrients causes instability and possibly the extinction of species.

Furthermore, this example shows that the higher codimension bifurcations can easily be spotted once the full parameter dependence of the bifurcation surfaces is known. In the three-parameter bifurcation diagram, codimension-2 bifurcations appear as lines at which codimension-1 surfaces intersect (DH, GG) or meet (TB) each other. Codimension-3 bifurcations are generally expected to appear as points. The appearance of what seems to be a line of codimension-3 bifurcations at $a = 0$ is caused by the well-known degeneracy of food chains of Lotka–Volterra type.

5. Discussion

We have demonstrated that the proposed method is a valuable tool for the bifurcation analysis of ODE systems. In small systems ($N \leq 4$), the necessary calculations can usually be done with pen and paper. In this case, the method can be seen as a more convenient way of finding the bifurcation surfaces than working out the eigenvalues explicitly. One potential disadvantage of the method of resultants is that it only yields bifurcation surfaces, whereas by working out the eigenvalues, one can deduce the stability of the steady state as well. However, knowing the bifurcation surface, the stability on either side of the surface can be found by running a simulation or calculating the eigenvalues numerically at one point on each side of the surface. The two points needed can be chosen in a way that the eigenvalues can be guessed or the simulation runs smoothly.

For systems of intermediate size ($4 < N \leq 10$), one would normally resort to computational techniques. Resultants are rarely used since it is known that the computation of characteristic polynomial coefficients is numerically unstable. However, we propose to use resultants in an analytical, computer algebra assisted approach. The computation of polynomial coefficients is done analytically and therefore is not critical. Numerics is only needed to plot the implicit solutions. Although other formulations of resultants exist, the Sylvester resultant used here is advantageous. In our calculations, the two main steps, the calculation of the polynomial coefficients and the calculation of the resultant, are of equal complexity. This helps to keep the build-up of complexity of the solutions relatively low. Therefore, the method, including computational sampling of the implicit analytic solution, is in many cases faster and safer than fully computational approaches.

Consider furthermore that even for $N = 10$, the coefficients c_n with even n only occur four times in the resultant matrix. Therefore, the resultant is a polynomial of order 4 or less in these coefficients. Hence, it is always possible to derive an explicit function for the value of a given coefficient (say c_0) on the bifurcation surface. That allows one to plot the bifurcation surfaces without sampling the implicit solution if the parameters can be given as explicit functions of the c_n.

Another problem of the method presented here is that it depends on the knowledge of the steady state under consideration. It is therefore especially suited for cases in which the steady state is easy to obtain. In these cases, the method has several advantages. Most importantly, the implicit solution contains the full parameter dependence, which allows illustrative three-parameter bifurcation diagrams to be created easily. Higher codimension bifurcations, like Takens–Bogdanov, Gavrilov–Guckenheimer, or double Hopf bifurcations, and even codimension-3 bifurcations, turn up in a natural way. Furthermore, having an alternative method at hand is an advantage of its own, especially since the method is analytical and can therefore be successfully applied where other methods run into computational problems.

Although the proposed method is in principle still applicable for large systems ($N > 10$), the resultants involved tend to become too large to be handled easily with standard symbolic software. However, we believe

that this limit could be increased by using specialized programs employing parallel processing.

Finally, the method could (in spirit) be extended to cover other interesting situations as well. This is possible since every algebraic condition imposed on the eigenvalues of the Jacobian may be used to split the characteristic polynomial into a system of polynomials that may be solved using resultants. Unfortunately, the reduction of the order of the polynomial by a factor of two, which arose from the symmetry condition, is lost. Therefore, the method seems to be advantageous only for Hopf bifurcation and the related situations mentioned earlier. Nevertheless, this result implies that the dynamics around a steady state of an N-dimensional ODE system can always be described qualitatively in terms of N parameters (for instance, the characteristic polynomial coefficients $c_0, \ldots, c_{N-1}$) even if the model has many more parameters.

Acknowledgements

The authors would like to thank V.N. Belykh, W. Ebenhöh, B. Fiedler and L.P. Shil'nikov for valuable discussions. This work was supported by the Deutsche Forschungsgemeinschaft (FE 359/6).

References

[1] E. Hopf, Abzweigung einer periodischen Lösung von einer stationären Lösung eines Differentialgleichungssystems, Ber. Math-Phys. Sächs. Akad. Wiss. 94 (1942) 1.
[2] J. Neĭmark, On some cases of periodic motions depending on parameters, Dokl. Akad. Nauk. SSSR 129 (1959) 736.
[3] R.S. Sacker, On invariant surfaces and bifurcations of periodic solutions of ordinary differential equations, Commun. Pure Appl. Math. 18 (1965) 717.
[4] F.H. Busse, J.A. Whitehead, Oscillatory and collective instabilities in large Prandtl number convection, J. Fluid Mech. 66 (1974) 67.
[5] R.J. Field, E.Körös, R.M. Noyes, Oscillations in chemical systems. II. Thorough analysis of temporal oscillations in the bromate–cerium–malonic acid system, J. Am. Chem. Soc. 94 (1972) 8649.
[6] B. Hassard, Bifurcation of periodic solutions of the Hodgkin–Huxley model for the squid giant axon, J. Theor. Biol. 71 (1978) 401.
[7] S. Rahmsdorf, Bifurcations of the atlantic thermohaline circulation in response to changes in the hydrological cycle, Nature 378 (1995) 145.
[8] S. Titz, T. Kuhlbrodt, S. Rahmsdorf, U. Feudel, On freshwater-dependent bifurcations in box models of the interhemispheric thermohaline circulation, Tellus A 54 (2001) 89.
[9] J. Guckenheimer, P. Holmes, Nonlinear Oscillations, Dynamical Systems, and Bifurcations of Vector Fields, 7th ed., Springer, 2002.
[10] J. Argyris, G. Faust, M. Haase, An Exploration of Chaos: An Introduction for Natural Scientists and Engineers, North-Holland, 1994.
[11] M. Holodniok, M. Kubiček, New algorithms for the evaluation of complex bifurcation points in ordinary differential equations, a comparative numerical study, Appl. Math. Comput. 15 (1984) 261.
[12] D. Roose, An algorithm for computation of Hopf bifurcation points in comparison with other methods, J. Comput. Appl. Math. 12 (1985) 517.
[13] G. Pönisch, Ein implementierbares ableitungsfreies Verfahren zur Bestimmung von Rückkehrpunkten, Beitr. Numer. Math. 9 (1981) 147.
[14] E. Doedel, H.B. Keller, J.P. Kernevez, Numerical analysis and control of bifurcation problems. I. Bifurcations in finite dimensions, Int. J. Bifurc. Chaos 3 (1991) 493.
[15] U. Feudel, W. Jansen, Candys/qa—a software system for the qualitative analysis of nonlinear dynamical systems, Int. J. Bifurc. Chaos 2 (1992) 773.
[16] Y.A. Kuznetsov, Elements of Applied Bifurcation Theory, Springer, 1995.
[17] A. Back, J. Guckenheimer, M. Myers, F. Wicklin, P. Worfolk, dstool: computer assisted exploration of dynamical systems, Notices Am. Math. Soc. 39 (1992) 303.
[18] H.E. Nusse, J. Yorke, Dynamics: Numerical Explorations, Lecture Notes in Mathematics No. 1687, Springer, 1997.
[19] J. Guckenheimer, M. Myers, B. Sturmfels, Computing Hopf bifurcations I, SIAM J. Numer. Anal. 34 (1997) 1.
[20] P. Glendinning, Stability, Instability and Chaos: An Introduction to the Theory of Nonlinear Differential Equations, Cambridge University Press, 1994.
[21] B. Werner, Computation of Hopf bifurcation with bordered matrices, SIAM J. Numer. Anal. 2 (1996) 435.
[22] I.M. Gelfand, M.M. Kapranov, A.V. Zelevinsky, Discriminants, Resultants and Multidimensional Determinants, Birkhäuser, 1994.
[23] J. Guckenheimer, M. Myers, Computing Hopf bifurcations. II. Three examples from neurophysiology, SIAM J. Sci. Comput. 17 (1996) 1275.
[24] A.L. Shil'nikov, Homoclinic phenomena in laser models, Comput. Math. Appl. 34 (1997) 245.
[25] T. Shimizu, N. Morioka, On the bifurcation of a symmetric limit cycle to an asymmetric one in a simple model, Phys. Lett. A 76 (1980) 201.
[26] V.N. Belykh, Bifurcation of separatrices of a saddle point of the Lorenz system, MAIK Nauka/Interperiodica Publ. 20 (1984) 1184.
[27] D.L. DeAngelis, Dynamics of Nutrient Cycling and Food Webs, 1st ed., Chapman & Hall, 1992.
[28] M. Rosenzweig, Paradox of enrichment: destabilization of exploitation ecosystems in ecological time, Science 171 (1971) 385.